Open Journal of Inorganic Chemistry, 2016, 6, 1-14

http://dx.doi.org/10.4236/ojic.2016.61001

Analytical, Spectral, Thermal and Molecular Modeling Studies of Hg^{2+}-2,3-Butanedionemonoxime Girard's T Hydrazone Complex and Its Application

Najlaa S. Al-Radadi[1], Magda M. Akl[2], Mohamed A. Elbeshlawi[2], Mohsen M. Mostafa[2]*

[1]Chemistry Department, Faculty of Science, Taibah University, Al-Madinah, Saudia Arabia
[2]Chemistry Department, Faculty of Science, Mansoura University, Mansoura, Egypt
Email: *amohsenmostafa@yahoo.com

Received 28 September 2015; accepted 3 January 2016; published 6 January 2016

Abstract

The coordination behavior of 2,3-butanedionemonoxime Girard's T hydrazone (L^1) towards Hg^{2+} ion has been investigated. The structure of Hg^{2+} complex, $[Hg(L^1)Cl]Cl\cdot 5H_2O$, is elucidated using elemental analyses, spectral (IR, UV-visible, 1H-NMR and mass) and TGA measurements. IR spectrum suggests that L^1 behaves in a bidentate manner through the azomethine groups. The molecular modeling of L^1 and its Hg^{2+} complex has been investigated. The bond lengths, bond angles, HOMO and LUMO have been calculated. The thermal behavior and kinetic parameters are determined using Coats-Redfern method. The use of L^1 for preconcentration and separation via flotation of Hg^{2+} complex and determination using cold vapor atomic spectrometry (CVAAS) is described. The effects on the percentage of recovered Hg^{2+} by pH of sample solutions, oleic acid (HOL) concentration, Hg^{2+} and L^1 concentrations are studied in details. The method is applied for the determination of the total Hg^{2+} ($mg\cdot mL^{-1}$) in natural water samples.

Keywords

Mercury Complex, 2,3-Butanedionemonoxime Girard's T Hydrazone, Modeling, Spectral Studies, Separation Using Flotation Method

1. Introduction

Coordination compounds play a vital role in our lives and in various fields. Also, the complexes have the ability

---

*Corresponding author.

How to cite this paper: Al-Radadi, N.S., Akl, M.M., Elbeshlawi, M.A. and Mostafa, M.M. (2016) Analytical, Spectral, Thermal and Molecular Modeling Studies of Hg^{2+}-2,3-Butanedionemonoxime Girard's T Hydrazone Complex and Its Application. *Open Journal of Inorganic Chemistry*, **6**, 1-14. http://dx.doi.org/10.4236/ojic.2016.61001

to chelate metal ions via several sites such as nitrogen, oxygen, and/or sulfur atoms [1]. Recently, since the increasing use of coordination compounds in analytical, bio-, medicinal chemistry and pigments, many investigators are embarked to these topics, especially the important roles of the complexes derived from hydrazone-oximes. There has been considerable interest in the development of novel compounds with anticonvulsant, antidepressant, analgesic, anti-inflammatory, antiplatelet, antimalarial, antimicrobial, anti-mycobacterial, and anti-tumor, and vasodilator, antiviral and anti-schistosomiasis activities. Hydrazones possess azometine moiety, which constitutes an important class of compounds for new drug development. Therefore, many researchers direct to synthesize these classes of compounds as target structures and evaluate their biological activities. These observations have been guided for the development of new hydrazones that possess varied biological activities [2]. Mercury is a highly toxic element that is found both naturally and as an introduced contaminant in the environment. The risk is determined by the likelihood of exposure, the form of mercury present (some forms are more toxic than others) and the geochemical and ecological factors that influence how mercury moves and changes form in the environment. Numerous techniques for the separation and/or pre-concentration of trace metals from different analytes have been reported such as volatilization, liquid-liquid extraction, selective dissolution, precipitation, electrochemical deposition and dissolution, ion exchange, liquid chromatography, flotation, freezing and zone melting and cloud point extraction (CPE) [3]. Of these techniques flotation has the particular merit of providing efficient, quick, simple preconcentration of trace elements both as anionic or cationic species from: a) media of low and high salinity [4] and b) large solution volumes [5]; it therefore has a considerable potential in the determination of very small amounts of metal ions in solution. The flotation technique can be classified into precipitate flotation and ion flotation. In ion flotation technique, the desired trace ions in an aqueous solution are converted into hydrophobic species by adding ligands and/or surfactants floated with the aid of numerous bubbles and concentrated in a scum or copious foam layer on the solution surface [6].

The lack of any studies reported in literature concerning the synthesis and characterization of $[Hg(\mathbf{L^1})Cl]Cl\cdot5H_2O$ gives us the push to investigate the Hg^{2+} complex. Also, the aim of the present study is to throw more light on the synthesis and characterization of Hg^{2+} complex. Moreover, our goal is extended to introduce 2,3-butanedionemonoxime Girard's T hydrazone as a new reagent for the flotation and CVAAS determination of total Hg^{2+} traces in water samples. Finally, the different experimental factors affecting the flotation process have been investigated in details.

2. Experimental

2.1. Materials and Reagents

All the chemicals used were of analytical grade and used without further purification. A saturated solution of Hg^{2+} (1000 mg L^{-1}) was used after appropriate dilution with double deionized distilled water. Other chemicals and reagents were from BDH quality. Oleic acid (HOL) stock solution, 6.36×10^{-2} $mol\cdot dm^{-3}$ was prepared by dispersing 20 cm^3 of HOL, (food grade with sp. gr. 0.895, provided by JT Baker Chemical Co.), in 1 dm^3 kerosene. $\mathbf{L^1}$ was prepared as described earlier [7]. A Perkin-Elmer model 2380 AAS was used, inconnection with a mercury hydride system (MHS-10). Nitrogen or argon was used as a purge gas and $NaBH_4$ as reluctant. Elemental analyses (C, H, M) were performed with a Perkin-Elmer 2400 series II analyzer at the Microanalytical Center at Cairo University, Egypt. Chloride was determined gravimetrically the as AgCl [8]. The IR spectrum of $[Hg(\mathbf{L^1})Cl]Cl\cdot5H_2O$ was recorded as KBr discs on Mattson 5000 FTIR spectrophotometer (400 - 4000 cm^{-1}). ^{1}H-NMR spectra were recorded on Jeol-90Q Fourier Transform (200 MHz) in d_6-DMSO at Cairo University, Egypt. Mass spectra were recorded on MS 70 eV EIGC, MS QP-1000 EX Shimadzu (Japan) mass spectrometer at Cairo University. Thermal analyses measurements (TG, DTG) were recorded with a Shimadzu Thermo gravimetric Analyzer TGA-50 using α-Al_2O_3 as a reference material at Mansoura University.

2.2. Flotation Cells

Two types of flotation cells were used throughout this work have been described earlier [9]. Flotation cell (a) is a cylindrically graduated glass tube of 16 mm inner diameter and 290 mm length with a stopcock at the bottom. Such cell is used to study the different factors affecting the efficiency of flotation. Flotation cell (b) is a cylindrical tube of 6 cm inner diameter and 45 cm length with a stopcock at the bottom and a quick fit stopper at the top; this cell is used to separate mercury from 1 dm^3 of different water samples. The pH of each sample was adjusted in the range 2 - 10 using Hanna Instruments 8519 digital pH meter with glass and saturated calomelelectrodes calibrated on the operational state using standard buffer solutions.

2.3. Characterization

The structure of **L**^{1} and its Hg^{2+} complex, geometry optimization and conformational analysis has been performed using of MM^+ force field as implemented in Hyperchem 8.0 [10]. The low lying obtained from MM^+ was then optimized at PM3 using the Polak-Ribiere algorithm in RHF-SCF set to terminate at an RMS gradient of 0.01 $Kcal \cdot mol^{-1}$.

2.4. Analytical Procedures

Two mL of aqueous EtOH solution of 1×10^{-4} $mol \cdot L^{-1}$ and **L**^{1} were introduced into a flotation cell containing 1×10^{-6} mol^{-1} of Hg^{2+} solution then the pH was adjusted to 5.0 using HCl and/or NaOH and the solution was mixed thoroughly. The mixture was then diluted to 10 mL with redistilled water. To the above solution 3 mL of oleic acid with a definite concentration (2×10^{-4} $mol \cdot L^{-1}$) were added. The cell was then turned upside down twenty times by hand and kept upright for 5 min to ensure complete flotation of the Hg^{2+} complex species. The scum layer was eluted with 5 mL of L^1 $mol \cdot L^{-1}$ HCl (1:1) solution to complete trapping [11]. The concentration of Hg^{2+} was determined using CVAAS measurements at 253.7 nm with a Perkin-Elmer 2380 atomic absorption spectrometer. The separation efficiency (%F) was calculated from the relation:

$$\%F = \left(C_s / C_i \right) \times 100\%$$

where, C_s and C_i denote the scum and the initial concentrations of Hg^{2+}, respectively.

2.5. Analysis of Water Samples

Water samples were obtained as follows: distilled water, tap water, river Nile and underground water from Mansoura City. All samples were filtered through G_4 sintered glass. For total organic mercury in water, the samples were digested in a closed system using the sequence of 10 mL of 5% KMnO4, 10 mL of 8N HNO3, 10 mL of 18 N H_2SO_4 and 20 ml of 4% $K_2S_2O_8$. The samples were heated at <90˚C for 30 min, allowed to cool and then 4 mL of 10% $NH_2OH \cdot HCl$ was added to reduce excess oxidant immediately before the flotation procedure was carried out. To large flotation cells, five water samples (1 L each) containing a defined amount of Hg^{2+} chloride and 5 mL of 10^{-3} M **L**^{1} were added and the pH was adjusted to 5 - 6. The reaction mixture was shaken to ensure complete complex formation. Then, 8 mL 10^{-3} M HOL was added to each flotation cell and the cells are shaken upside down for five min. The scum layer was separated and eluted with 1 mol L^{-1} HCl. The final volume was 10 mL.

2.6. Synthesis of L^1

L^1($C_9H_{19}N_4O_2Cl$) was synthesized as described earlier [12] and can be represented by keto/enol forms as shown **Figure 1**. The product is white in color and soluble in H_2O and most polar organic solvents and the value of molar conductance in DMSO (28.3 $ohm^{-1} \cdot cm^2 \cdot mol^{-1}$) suggesting the electrolytic nature of **L**^{1}. The structure of **L**^{1} is confirmed using elemental analyses (Calcd: C = 40.2, H = 7.9, Cl = 13.2; Found: 40.4, 7.3, 12.9) and spectral measurements.The melting point of **L**^{1} is 172˚C, which matches the results reported value [12].

2.7. Synthesis and Characterization of [Hg(L^1)Cl]Cl·5H$_2$O

The Hg^{2+} complex, [Hg(**L**^{1})Cl]Cl·5H_2O, was synthesized by refluxing solutions of equivalent amounts of **L**^{1} and

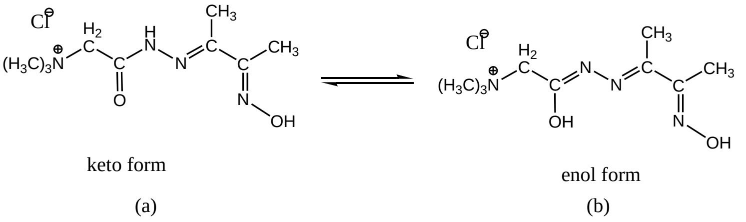

Figure 1. The keto and enolforms of **L**^{1}.

$HgCl_2$ in absolute EtOH for 0.5 h. The product was filtered off, washed several times with hot EtOH and Et_2O and finally dried in a vacuum desiccator over anhydrous $CaCl_2$. The yield of the Hg^{2+} complex is 96%. The structure of the complex is confirmed by its melting point (212˚C) and elemental analyses (Calcd: C = 17.7, H = 4.8, Hg = 32.7, Cl = 17.4; Found: 16.9, 4.8, 32.4 and 18.1) and represented in **Figure 2**.

3. Results and Discussion

3.1. Infrared Spectra

The IR spectrum of the free $\mathbf{L^1}$ (**Figure 1(a)**) in KBr shows a strong band at 1697 cm^{-1} assignable to the ν(C=O) vibration [13] in addition to medium and weak bands at 1650, 1614, 1405 and 1020 cm^{-1} assigned to the azomethine of hydrazone $\nu(C=N^1)$, azomethine of oxime $\nu(C=N^2)$, δ(OH) and ν(N-N) vibrations, respectively [14]. Also, the two bands observed at 3124 and 3214 cm^{-1} are assigned to the free ν(NH) and hydrogen bonded, respectively. The bands observed at 3395 and 3454 cm^{-1} are attributed to the (OH) free and bonded hydrogen, respectively. The broad weak bands in the 1800 - 1200 cm^{-1} and 2200 - 2400 cm^{-1} regions are taken as an evidence for the existence of intra-molecular hydrogen bonding of the type (OH… N) (**Figure S1**) [15].

The IR spectrum of $[Hg(\mathbf{L^1})Cl]Cl\cdot5H_2O$ (**Figure 3**) suggests that $\mathbf{L^1}$ coordinates as a neutral bidentate via the two azomethine groups as shown in **Figure 2**. The mode of chelation is supported by the IR spectrum where; i) the negative shift of both the bands of azomethine $(C=N^1)$ and $(C=N^2)$ groups and ii) the bands of the (C=O) and (OH) groups remainexisted after coordination indicating that these groups are not participated in the coordination.

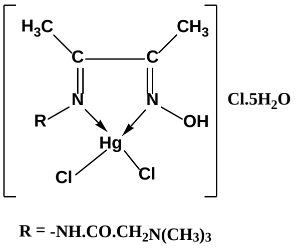

Figure 2. Structure of Hg^{2+} complex.

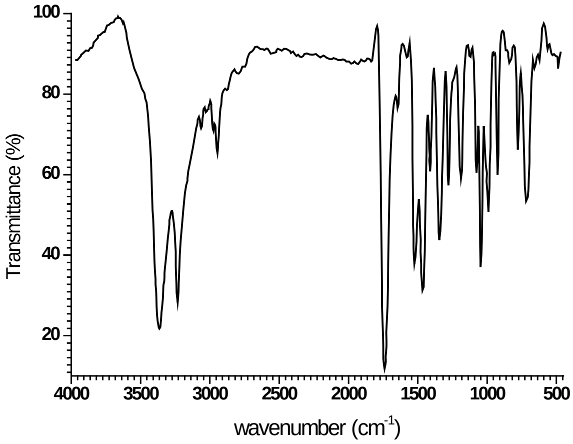

Figure 3. IR spectrum of $[Hg(\mathbf{L^1})Cl]Cl\cdot5H_2O$.

3.2. ¹H-NMR Spectra

The ^{1}H-NMR spectrum of $\mathbf{L^1}$ in d_6-DMSO (**Figure 4**) shows two signals at 11.74 ppm and 11.25 ppm, downfield with respect to TMS, which disappear upon adding D_2O. These signals are attributed to the protons of (OH) of the oxime group and (CONH) group, respectively. The signals in the 1.98 - 2.19 ppm range are assigned to the three methyl groups $(CH_3)_3$. Also, the signals observed at 2.50, 4.56 and 4.76 ppm are attributed to the protons of

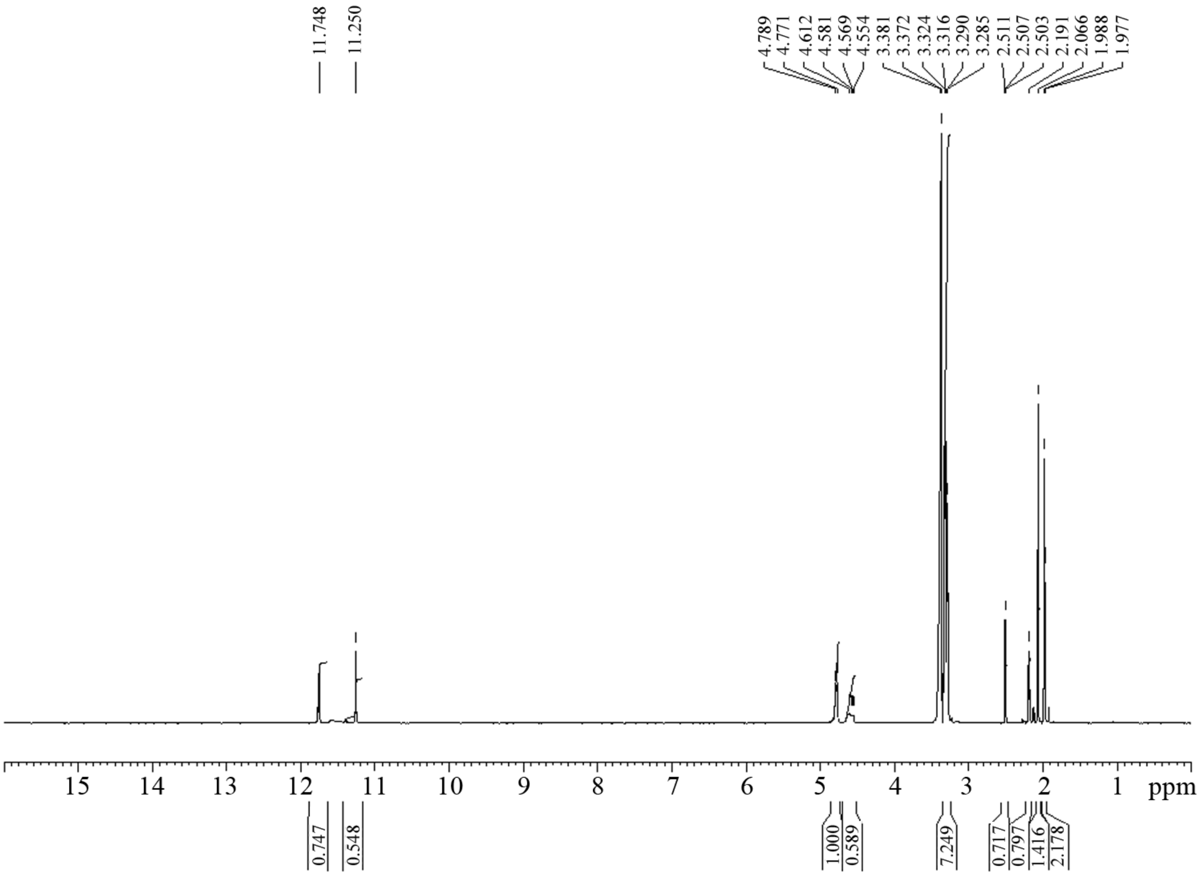

Figure 4. ^{1}H-NMR spectrum of $\mathbf{L^1}$ in d_6-DMSO and D_2O.

(CH_3) and (CH_2) of the oxime group and (CH_3) of the hydrazone group, respectively. All these foundations are taken as evidence that $\mathbf{L^1}$ is mainly existed in the keto form either in the free case or in the hydrogen bonded.

The ^{1}H-NMR spectrum of $[Hg(\mathbf{L^1})Cl]Cl\cdot5H_2O$ in d_6-DMSO (**Figure S2**) shows two signals at 11.73 ppm and 11.24 ppm, downfield with respect to TMS, which disappear upon adding D_2O (**Figure S3**). These signals are attributed to the protons of (OH) of the oxime and the NH of the (CONH) group, respectively. The signals in the 1.97 - 2.12 ppm range correspond to the three methyl groups $(CH_3)_3$. Also, the observed signals at 2.49 - 2.51 ppm, 4.3 ppm and 4.72 ppm are attributed to the protons of (CH_2) and (CH_3) of the oxime group and (CH_3) of the hydrazone group, respectively. All these observations confirm that the complex exists in the keto form**.**

3.3. Mass Spectra

The mass spectrum of $\mathbf{L^1}$ (**Figure S4**) shows the molecular ion peak at m/z = 250. This suggests that the proposed structure for $\mathbf{L^1}$ is correct and has the chemical formula; $C_9H_{19}N_4O_2Cl$ and the M. wt. = 250.726. Also, the results of elemental analyses and ^{1}H-NMR are taken as strong evidences for the proposed structure (**Figure 2**). The mass fragments of $\mathbf{L^1}$ are shown in **Scheme S1**. The mass spectrum of $[Hg(\mathbf{L^1})Cl]Cl\cdot5H_2O$ (**Figure S5**) shows the molecolare ion peak at m/z = 613 while the theoretical value is 612.29.

3.4. Molecular Modeling

The molecular modeling along with atom member of $\mathbf{L^1}$ and its Hg^{2+} complex, $[Hg(\mathbf{L^1})Cl]Cl\cdot5H_2O$, are shown in **Figure 5** and **Figure 6**. The data are calculated using quantum mechanics for the complexes. Semi-empirical molecular Mechanics Optimization method is used.

The data listed in **Table S1** and **Table S2** reveals the following remarks:

1) Some bond lengths don't change as in N(8)-O(20) of $\mathbf{L^1}$, N(3)-O(13) of complex, N(7)-N(13) of $\mathbf{L^1}$ and

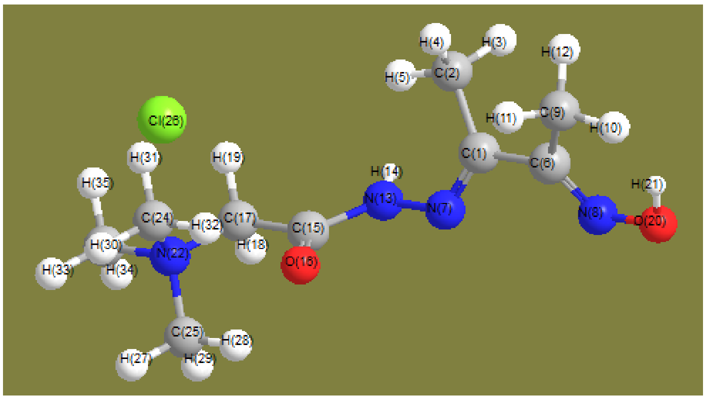

Figure 5. Molecular modeling of $\mathbf{L}^1$.

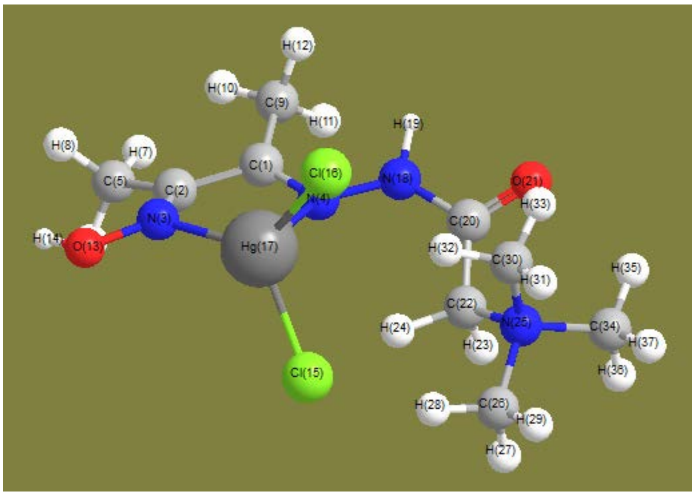

Figure 6. Modeling structure of $[Hg(\mathbf{L}^1)Cl]Cl\cdot 5H_2O$.

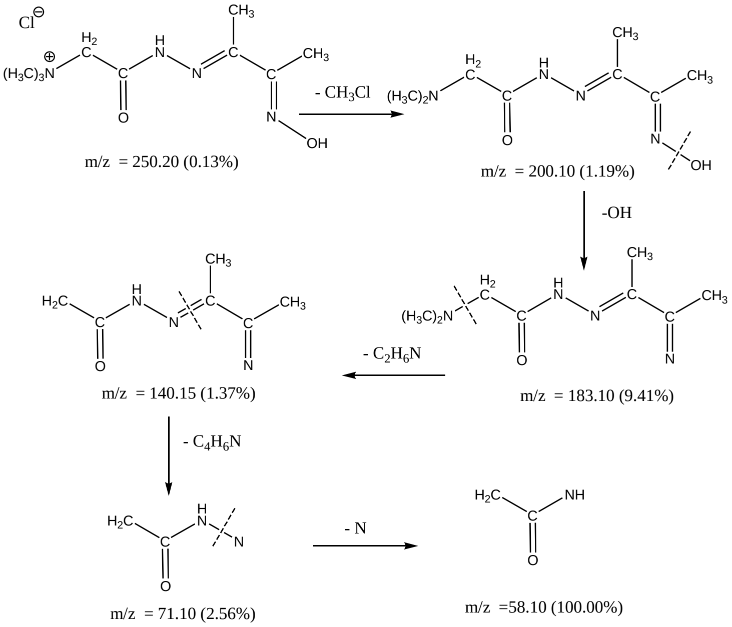

Scheme S1. The fragmentation pattern of $\mathbf{L}^1$.

N(4)-N(15) of complex which have the same values 1.316 Å and 1.352 Å, respectively.

2) On the other hand, some bonds are elongated as C(1)-N(7) and C(6)-N(8) of $\mathbf{L^1}$ (1.244 Å) but C(1)-N(4) and C(2)-N(3) of complex (1.377 Å).

3) Other bonds are shortened as C(1)-C(2) of $\mathbf{L^1}$ (1.540 Å) changed into 1.337 Å in the complex.

4) The same notifications can be discussed in bond angles. These differences take place on coordination and formation of the five-membered ring, which ensures the minimum energetic state of the complex.

3.5. Thermo Gravimetric Analysis

Thermal studies of the Hg^{2+} complex is studied in the range 30˚C - 800˚C to insight about its thermal stability, the nature of the solvent molecules and the general scheme for their thermal decomposition. The data showed that the water of crystallization is volatilized within the temperature range 75˚C - 125˚C. The TGA decomposition steps with the temperature range and weight loss for the Hg^{2+} complex.

3.6. Kinetic Studies

The kinetic parameters evaluated by Coats-Redfern method (**Figure 7**) are listed in **Table 1**. The data reveals the following observations:

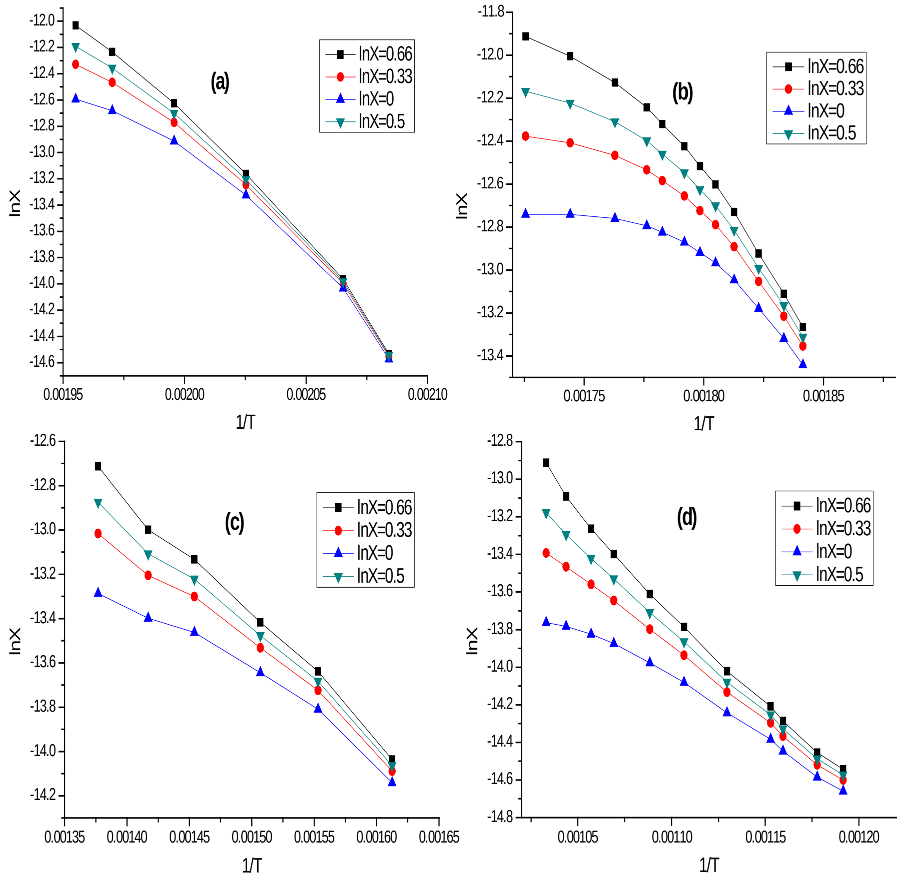

Figure 7. Modeling structure of $[Hg(\mathbf{L^1})Cl]Cl\cdot5H_2O$.

Table 1. Some of energetic properties of $\mathbf{L^1}$ calculated by $DMOL^3$ using DFT-method.

Compound	Total Energy (Kcal/mol)	Binding Energy (Kcal/mol)	Electronic Energy (Kcal/mol)	Hydration Energy (Kcal/mol)	Heat of Formation (Kcal/mol)	HOMO (eV)	LUMO (eV)
$\mathbf{L^1}$	−49870.05	−1465.47	−236244.78	−6.61	472.77	−10.2561	−2.2363

1) All decomposition stages showed a best fit for n = 1, while the other values have no better correlation.

2) The activation energy (E_a) decreases for the subsequent degradation steps revealing a less energy needed for the thermal decomposition of the remaining parts.

3) The negative value of the entropy of activation (ΔS*) of the decomposition steps of the metal complex indicates that the activated fragments have more ordered structure than the undecomposed complex and/or the decomposition reactions are slow [16].

4) The negative sign of the enthalpy of activation ΔH* of the decomposition stages reveals that the decomposition stages are easier.

The positive sign of free energy of activation (ΔG*) indicates that the free energy of the final residue is higher than that of the initial compound and hence all the decomposition steps are nonspontaneous processes. Moreover, the values of ΔG* increase significantly for the subsequent decomposition stages of a given compound. This conclusion, as a result of the increasing of TΔS* reflects that the rate of removal of the subsequent species is lower than that of the precedent one [17]-[19].

3.7. Analytical Studies

3.7.1. Influence of pH

The pH of a solution is a very important factor for metal chelate formation and for the flotation process. Therefore, the effect of pH on the flotation of Hg-**L**^{1} chelate was studied in the pH values ranging from 2.0 to 9.0. The results are shown in **Figure 8**. In the absence of **L**^{1} (**Figure 8(a)**) the flotation efficiency of Hg^{2+} is very low over the pH range tested. The maximum flotation efficiency (~92%) was recorded over pH values ranging from 4.5 to 6.0. According to **Figure 8** (A andb) the effective role of **L**^{1} is clear; it forms a complex with Hg^{2+} ions rendering them more hydrophobic and easily separated from the solution bulk using the HOL surfactant. At higher pH valuesthe decrease in the flotation efficiency is attributed to the formation of a white emulsion and due to the formation of excessive foams of sodium oleate. This will hinder the reaction to complete.

3.7.2. Influence of Oleic Acid Concentration [HOL]

The surfactant concentration (oleic acid) is very important parameter; up to a certain concentration of HOL the floatability increase. **Figure 9** shows that the floatability remains at higher up to value (~99%) over the concentration range (2 - 6 × 10^{-4} mol·L^{-1}) of oleic acid and decreases gradually as the concentration increases. The decrease in the flotation efficiency at higher HOL concentrations is due to the collection of the surfactant molecules together forming micelles [6]. These micelles compete with colligend molecule, [Hg(**L**^{1})Cl]Cl·5H_2O and since they stay in the solution, they reduce the effectiveness of separation. In addition, the concentration of surfactant changes the bubble size with the size getting smaller as the surfactant increases.

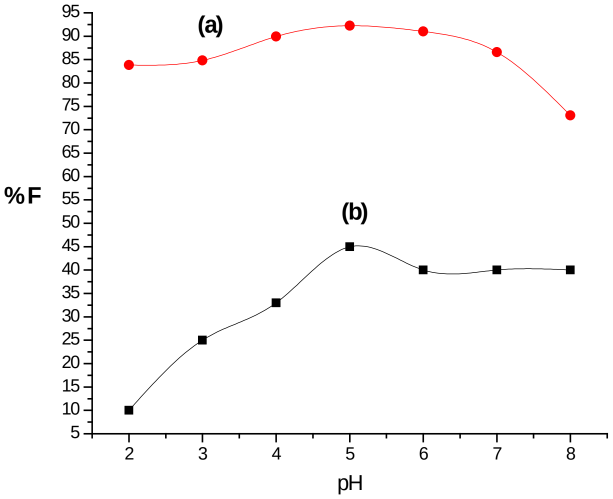

Figure 8. Influence of pH on the flotation efficiency of Hg (II): (a) in absence of **L**^{1} and (b) in the presence of 1.0 × 10^{-4} mol·L^{-1} L^1 and 2 × 10^{-4} mol·L^{-1}/HOL.

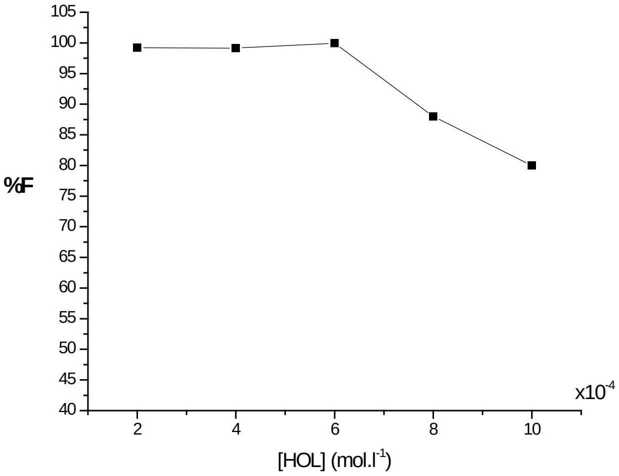

Figure 9. Influence of oleic acid (HOL) concentration on the flotation efficiency of Hg (II).

3.7.3. Influence of Ligand Concentration (L^1)

On fixing the various optimum conditions, the variety of **L^1** concentration was examined. The data obtained show that the floatability of the Hg^{2+} ion increases clearly reaching its maximum percentage (99%) at M:L ratio of (1:1). Moreover, excess amount of collector has no effect on the flotation process. Therefore, a concentration of 1×10^{-4} mol·L^{-1} **L^1** was used.

3.7.4. Influence of Temperature

The maximum flotation efficiency is obtained in the range (25˚C - 50˚C). The proposed flotation procedure is performed at room temperature (25˚C).

3.7.5. Influence of Volume

A series of experiments was achieved to float different concentrations of Hg^{2+} solution from different aqueous volumes using suitable large flotation cells under the recommended conditions. The results obtained revealed that, up to 30 µg of Hg^{2+} could be quantitatively separated from one liter into 10 mL of HOL with a preconcentration factor of 100.

3.7.6. Influence of Ionic Strength

Table 2 illustrates the effect of varying the ionic strength of different salts on the floatation efficiency of the studied metal ion using the optimum conditions. The salts used in adjusting the ionic strength generally similar natural water samples. It is quite clear that the ionic strength of the medium has not markedly affected the flotation process.

3.7.7. Influence of Foreign Ions

In order to study the tendency of **L^1** to form complexes with number metal ions, the effect of foreign metal ions on the flotation of Hg^{2+} ion using the optimum conditions is examined. These foreign ions are selected on the basis that they are normally present in fresh and saline waters. The tolerable amounts of each ion giving a maximum error ±5% in the flotation efficiency are summarized in **Table 3**. The experimental data showed that most of the investigated foreign cations (Na^+, K^+, Ca^{2+} and Mg^{2+}) and anions (acetate, oxalate, Cl^-, I^-, PO_4^{3-}, NO_3^- and ClO_4^-) did not interfere in the recovery of Hg^{2+} ion using the optimum conditions whereas other foreign ions have little interfering effects (~2%). All of these interferences were completely removed by increasing the concentration of **L^1**.

3.7.8. Mechanism of Flotation

The nature of the interaction between oleic acid surfactant and the formed complex must be studied to approach the actual mechanism of flotation. The proposed mechanism may proceed through: i) a physical interaction; ii)

Table 2. Influence of ionic strength on the flotation (% F) of Hg^{2+}.

Salt	Concentration, $mol \cdot L^{-1}$	F %
NaCl	0.01	99.98
	0.05	99.02
	0.10	98.77
KNO_3	0.01	99.98
	0.05	98.82
	0.10	98.54
$CaCl_2$	0.01	99.98
	0.05	97.99
	0.10	97.73

Table 3. Influence of foreign ions on the floatability of Hg^{2+} under the optimum conditions.

Ion	Concentration, $mg \cdot L^{-1}$	F %
K^+	1×10^4	100.00
Na^+	1×10^4	99.98
Ca^{2+}	1×10^3	99.98
Mg^{2+}	1×10^3	98.49
Al^{3+}	10	98.00
Cu^{2+}	0.2	96.47
Co^{2+}	0.2	97.49
Mn^{2+}	0.2	97.38
Hg^{2+}	0.2	98.74
CH_3COO^-	0.5	99.15
Oxalate	0.5	99.01
Cl^-	0.5	99.36
I^-	0.5	98.95
PO_3^{3-}	0.5	98.39
NO_3^-	0.5	98.99
ClO_4^-	0.5	99.00

Table 4. Removal of Hg^{2+} from water samples ($\mathbf{L}^1$ = 10 - 3 M, pH = 5, 25˚C, n = 3).

Water sample	$Hg^{2+}/\mu g \cdot mL^{-1}$		Recovery (%)
	Added	Found	
Distilled water	0.5	0.49	98
	1.0	1.0	100
Tank water (Mansoura city)	0.5	0.50	100
	1.0	1.01	101
Nile water (Mansoura city)	0.5	0.48	96
	1.0	0.98	98
Underground water (Mansoura city)	0.5	0.46	92
	1.0	0.96	96

by forming a hydrogen bond between the hydrophilic part of HOL and the active sites in the ligand complex or iii) by an interaction between oleic acid and the complex, formed in solution through a coordinate bond forming a self-floatable (Hg^{2+}-$\mathbf{L}^1$-HOL) species. In all cases, the hydrophobic part of the surfactant attaches to air bubbles and floats separating the analyte containing species.

3.7.9. Analytical Application

The determination of the Hg^{2+} ion in natural water samples was carried out by CVAAS after the flotation preconcentration was carried out. The samples were collected from different places. The analytical results are summarized in **Table 4**.

References

[1] Chaudhary, R. and Shelly (2010) Synthesis and Characterization of Cr (III), Fe (III) and Co (III) Complexes with Biacetyl and Bibenzoyl Monoxime Hydrazine. *Journal of Chemical and Pharmaceutical Research*, **2**, 707-713.

[2] Rollas Sand Küçükgüzel, Ş.G. (2007) Biological Activities of Hydrazone Derivatives. *Molecules*, **12**, 1910-1939. http://dx.doi.org/10.3390/12081910

[3] Mizuike, A. and Fresenius, Z. (1986) Preconcentration Techniques for Inorganic Trace Analysis. *Analytical Chemistry*, **324**, 672-677. http://dx.doi.org/10.1007/BF00468377

[4] Gabezon, L.M., Caballero, M., Cela, R. and Perez-Bustmante, J.A. (1984) Simultaneous Separation of Copper, Cadmium and Cobalt from Sea-Water by Co-Flotation with Octadecylamine and Ferric Hydroxide as Collectors. *Talanta*, **31**, 597-602. http://dx.doi.org/10.1016/0039-9140(84)80176-9

[5] Feng, X. and Ryan, D.E. (1984) Combination Collectors in Adsorption Colloid Flotation Formultielement Determination in Waters by Neutron Activation. *Analytica Chimica Acta*, **162**, 47-55. http://dx.doi.org/10.1016/S0003-2670(00)84226-9

[6] Akl, M.A. (2006) The Use of Phenanthraquinone Monophenyl Thiosemicarbazone for Preconcentration, Ion Flotation and Spectrometric Determination of Zinc (II) in Human Biofluids and Pharmaceutical Samples. *Bulletin of the Korean Chemical Society*, **27**, 725-732. http://dx.doi.org/10.5012/bkcs.2006.27.5.725

[7] Ghazy, S.E. and Kabil, M.A. (1994) Determination of Trace Copper in Natural Waters after Selective Separation by Flotation. *Bulletin of the Chemical Society of Japan*, **67**, 2098-2102. http://dx.doi.org/10.1246/bcsj.67.2098

[8] Vogel, A.I. (1994) A Text Book of Quantitative Inorganic Chemistry. Longmans, London.

[9] Khalifa, M.E., Akl, M.A. and Ghazy, S.E. (2001) Selective Flotation-Spectrophotometric Determination of Trace Copper (II) in Natural Waters, Human Blood and Drug Samples Using Phenanthraquinone Monophenyl Thiosemi Carbazone. *Chemical and Pharmaceutical Bulletin*, **49**, 664-668. http://dx.doi.org/10.1248/cpb.49.664

[10] Coggon, P., Mcphail, A.T., Mabbs, F.E., Richards, A. and Thornley, A.S. (1970) Preparation, Magnetic, and Electronic Spectral Properties of Some Chromium(III)—*NN*'-Ethylenebis (Salicylideneiminato) Complexes: Crystal and Molecular Structure of *NN*'-Ethylenebis (Salicylideneiminato) Diaquochromium (III) Chloride. *Journal of the Chemical Society A*, **1970**, 3296-3303. http://dx.doi.org/10.1039/j19700003296

[11] Marczenko, Z. (1986) Separation and Spectrophotometric Determination of Elements. John Wiely& sons, Toronto.

[12] Mostafa, M.M., Hassan, S.M. and Ibraheim, G.M. (1980) Copper Complexes of Diacetylmonoxime Girard T. *Journal of Inorganic and Nuclear Chemistry*, **42**, 285-286. http://dx.doi.org/10.1016/0022-1902(80)80259-4

[13] Coygon, P., Mcphail, A.T., Mabbs, F.E., Richards, A. and Thornley, A.S. (1970) Preparation, Magnetic, and Electronic Spectral Properties of Some Chromium(iii)-N''-Ethylenebis(salicylideneiminato) Complexes: Crystaf and Molecular Structure of NN'-Ethylenebis(sa1icy1 ideneiminat0)diaquochromium(iii) Chloride. *Journal of the Chemical Society A*: *Inorganic*, *Physical*, *Theoretical*, **1970**, 3296-3303.

[14] Nakamoto, K. (2009) Infrared and Raman Spectra of Inorganic and Coordination Compounds. John Wiley and Sons Inc., 58B.

[15] Bullock, J.I. and Tajmir-Riahi, H.A. (1978) Schiff-Base Complexes of the Lanthanoids and Actinoids. Part 1. Lanthanoid (III) Halide Complexes with the Un-Ionised form of NN'-Ethylenebis (Salicylideneimine) and Related Bases. *Journal of the Chemical Society*, *Dalton Transactions*, **1**, 36-39. http://dx.doi.org/10.1039/dt9780000036

[16] Frost, A.A. and Pearson, R.G. (1961) Kinetics and Mechanisms. Wiley, New York.

[17] Maravalli, P.B. and Goudar, T.R. (1999) Thermal and Spectral Studies of 3-*N*-Methyl-morpholino-4-amino-5-mercapto-1,2,4-triazole and 3-*N*-methyl-piperidino-4-amino-5-mercapto-1,2,4-triazolecomplexes of Cobalt (II), Nickel (II) and Copper (II) Thermo. *Chimica Acta*, **325**, 35-41. http://dx.doi.org/10.1016/S0040-6031(98)00548-6

[18] Yusuff, K.K.M. and Sreekala, R. (1990) Thermal and Spectral Studies of 1-Benzyl-2-phenylbenzimidazole Complexes of Cobalt (II) Thermo. *Chimica Acta*, **159**, 357-368. http://dx.doi.org/10.1016/0040-6031(90)80121-E

[19] Kandil, S.S., El-Hefnawy, G.B. and Baker, E.A. (2004) Thermal and Spectral Studies of 5-(Phenylazo)-2-thiohydantoin and 5-(2-Hydroxyphenylazo)-2-thiohydantoin Complexes of Cobalt (II), Nickel (II) and Copper (II) Thermo. *Chimica Acta*, **414**, 105-113. http://dx.doi.org/10.1016/j.tca.2003.11.021

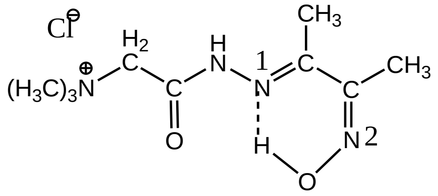

Figure S1. Intra-molecular hydrogen bonding in $\mathbf{L^1}$.

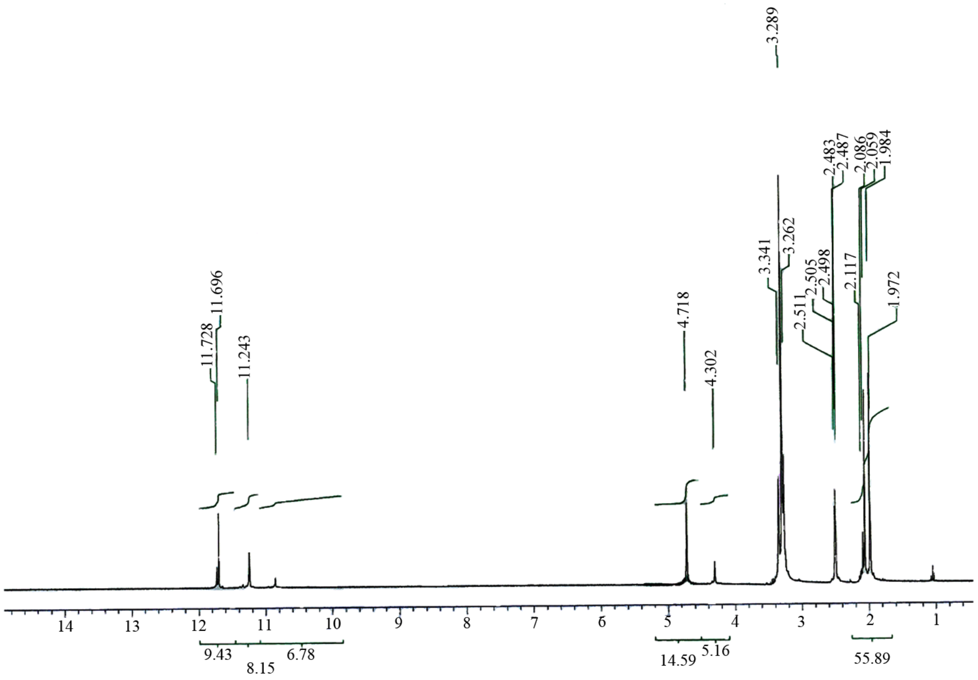

Figure S2. ^{1}H-NMR spectrum of [Hg(L^1)Cl]Cl·5H_2O in d_6-DMSO.

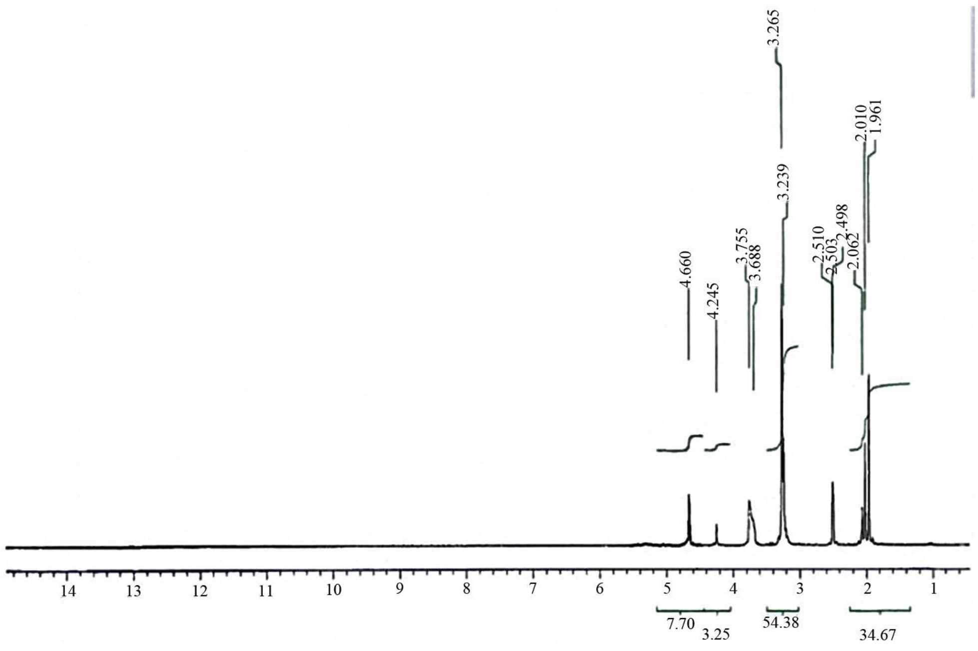

Figure S3. ^{1}H-NMR spectrum of [Hg($\mathbf{L^1}$)Cl]Cl·5H_2O in d_6-DMSO and D_2O.

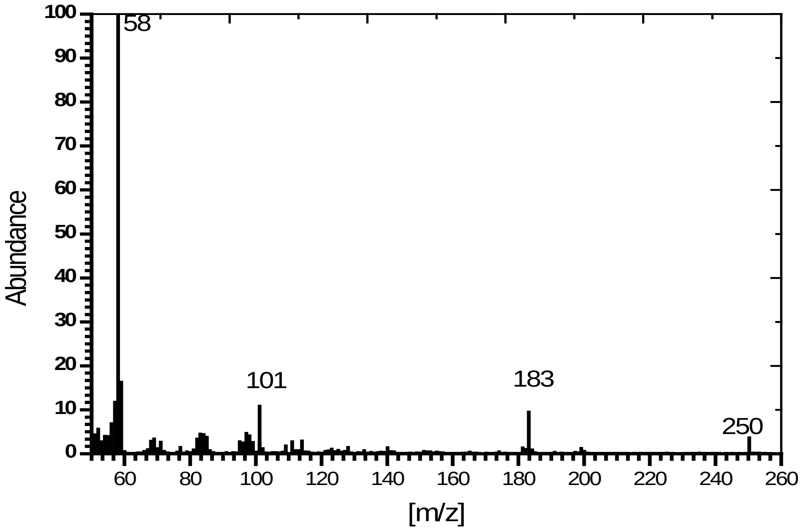

Figure S4. Mass spectrum of L^1.

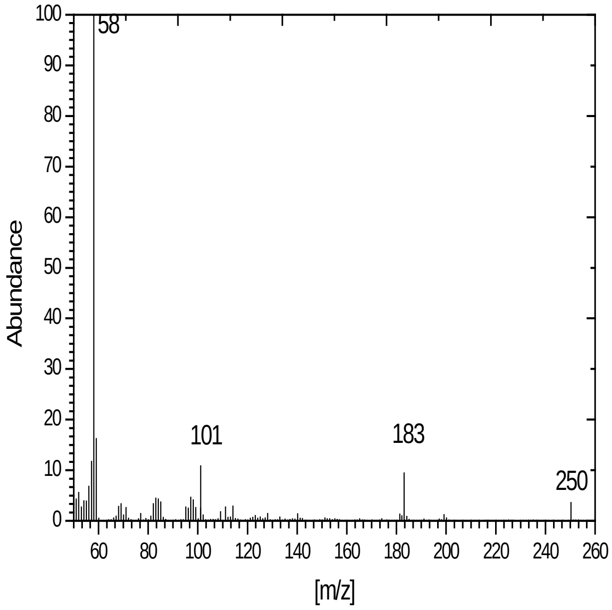

Figure S5. Mass spectrum of $[Hg(\mathbf{L^1})Cl]Cl\cdot 5H_2O$.

Table S1. Bond length of $\mathbf{L^1}$.

Bond	Length (Å)	Bond	Length (Å)	Bond	Length (Å)
C(1)-C(2)	1.540	N(13)-H(14)	1.028	O(20)-H(21)	0.992
C(1)-C(6)	1.540	N(7)-N(13)	1.352	N(22)-C(23)	1.446
C(1)-N(7)	1.244	N(8)-O(20)	1.316	N(22)-C(24)	1.446
C(6)-N(8)	1.244	N(13)-C(15)	1.446	N(22)-C(25)	1.446
C(6)-C(9)	1.540	N(13)-H(14)	1.028	C(17)-N(22)	1.446
N(7)-N(13)	1.352	C(15)-O(16)	1.213	N(13)-C(15)	1.446
N(8)-O(20)	1.316	C(15)-C(17)	1.540	——	——

Table S2. Bond angle of BMGT.

Angle	Angle (˚)	Angle	Angle (˚)
C(2)-C(1)-C(6)	119.999	N(13)-C(15)-O(16)	119.999
C(2)-C(1)-N(7)	119.999	N(13)-C(15)-C(17)	120.000
C(6)-C(1)-N(7)	120.000	O(16)-C(15)-C(17)	119.999
C(1)-C(6)-N(8)	120.000	C(15)-C(17)-N(22)	109.500
C(1)-C(6)-C(9)	119.999	N(8)-O(20)-H(21)	109.500
N(8)-C(6)-C(9)	119.999	C(17)-N(22)-C(23)	109.500
C(1)-N(7)-N(13)	120.000	C(17)-N(22)-C(24)	109.500
C(6)-N(8)-O(20)	120.000	C(17)-N(22)-C(25)	109.500
N(7)-N(13)-C(15)	120.000	C(23)-N(22)-C(24)	109.500
N(7)-N(13)-H(14)	119.999	C(23)-N(22)-C(25)	109.500
H(14)-N(13)-C(15)	119.999	C(24)-N(22)-C(25)	109.327